Supergalactic Structure of Multiplets with the Telescope Array Surface Detector

Jon Paul Lundquist[1,*] and *Pierre V.* Sokolsky[1] on behalf of the Telescope Array collaboration

[1]High Energy Astrophysics Institute and Department of Physics and Astronomy, University of Utah, Salt Lake City, Utah, USA

Abstract. Evidence of supergalactic structure of multiplets has been found for ultra-high energy cosmic rays (UHECR) with energies above 10^{19} eV using 7 years of data from the Telescope Array (TA) surface detector. The tested hypothesis is that UHECR sources, and intervening magnetic fields, may be correlated with the supergalactic plane, as it is a fit to the average matter density within the GZK horizon. This structure is measured by the average behavior of the strength of intermediate-scale correlations between event energy and position (multiplets). These multiplets are measured in wedge-like shapes on the spherical surface of the field-of-view to account for uniform and random magnetic fields. The evident structure found is consistent with toy-model simulations of a supergalactic magnetic sheet and the previously published Hot/Coldspot results of TA. The post-trial probability of this feature appearing by chance, on an isotropic sky, is found by Monte Carlo simulation to be $\sim 4.5\sigma$.

1 Introduction

The supergalactic plane (SGP) is the average matter distribution of the local universe up to a distance of ~200 Mpc (a large percentage is within the GZK cutoff of 100 Mpc) [1]. Large scale magnetic fields are known to exist between some clusters of galaxies which make up the supergalactic plane such as the Coma Cluster [2]. And it has been shown that ~90% of the baryonic mass of the universe is between galaxies of which ~40% is warm-hot protons outside gas clouds [3]. This may allow the formation of intra-galactic large scale magnetic fields ([4],[5]).

The presence of large scale magnetic fields suggest that energy dependent deflection of ultra-high energy cosmic rays (UHECR) should appear correlated with the SGP. Previous energy-position correlation studies have not had significant results ([6],[7],[8]). These multiplet searches for significant small scale magnetic deflection patterns included scanned parameters chosen by assumed magnetic field models and compositions. This analysis uses intermediate-scale energy-position correlations to look for significant large scale magnetic structure and minimal assumptions are made regarding particular magnetic field models or composition.

2 Energy-Position Correlations

It is assumed that UHECR travel through uniform fields, approximated by Equation 1a, and random fields where the root mean squared deflection is approximated by Equation 1b (Z is mass number, S angular distance, B field strength, E energy, and L_c is mean magnetic field coherence length). It follows trivially that lower energy cosmic ray events are deflected to larger angles from a source than those with higher energy [9]. This drift-diffusion process, where high energy events are deflected from a source less than lower energy events, is diagrammed in Figure 1.

$$\delta \approx 0.5^\circ Z \frac{S}{\mathrm{kpc}} \frac{B}{\mu\mathrm{G}} \frac{10^{20}\mathrm{eV}}{E} \tag{1a}$$

$$\delta_{rms} \approx 0.1^\circ Z \frac{B_{rms}}{\mu\mathrm{G}} \frac{10^{20}\mathrm{eV}}{E} \sqrt{\frac{S}{\mathrm{kpc}}} \sqrt{\frac{L_c}{100\mathrm{pc}}} \tag{1b}$$

2.1 Correlation

The angular distance between two points on a sphere is the great circle distance (Equation 2 for normal vectors). Correlations between energy and angular distance are found using Kendall's τ_b ranked correlation that measures monotonic dependence [10]. Ranked correlation removes magnetic model and composition assumptions and also detector exposure effects on the correlation strength.

$$\delta_{ij} = \arctan \frac{|\hat{\mathbf{n}}_\mathbf{i} \times \hat{\mathbf{n}}_\mathbf{j}|}{\hat{\mathbf{n}}_\mathbf{i} \cdot \hat{\mathbf{n}}_\mathbf{j}} \tag{2}$$

The simplified τ_a, not taking into account duplicate values, is shown in Equation 3 for brevity. The difference between τ_a and τ_b in this analysis is small. Ranks are the ordering of a sorted variable (1st, 2nd, etc.). A pair of observed ranks (x_i, y_i) and (x_j, y_j) are concordant if $x_i > x_j$ and $y_i > y_j$ (or the converse). They are discordant if $x_i > x_j$ and $y_i < y_j$ (or the converse).

$$\tau_a = \frac{(\#\ concordant\ pairs) - (\#\ discordant\ pairs)}{n(n-1)/2} \tag{3}$$

*e-mail: jplundquist@cosmic.utah.edu

© The Authors, published by EDP Sciences. This is an open access article distributed under the terms of the Creative Commons Attribution License 4.0 (http://creativecommons.org/licenses/by/4.0/).

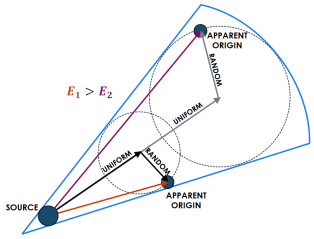

(a)

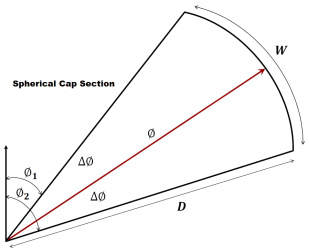

(b)

Figure 1. Drift-diffusion deflection of UHECR from a source. (a) Two events having traveled through uniform and random magnetic fields. The purple vector represents the lower energy event spherical arc and the red vector is a higher energy event. Random and uniform field components describe the average magnetic field perpendicular to the surface of the field of view (FOV) sphere. Dashed circles represent possible random field deflections. (b) A spherical cap section, "wedge," best encompasses the likeliest positions. Pointing direction is the spherical arc ϕ, width is $\Delta\phi$, and D is the maximum angular distance.

For a correlation of -1 (perfect discordance) an increase (decrease) of x always follows a decrease (increase) in y. For $+1$ (perfect concordance) an increase (decrease) of x always follows an increase (decrease) of y.

The pre-trial significance of a correlation (probability of τ_b=0 with infinite samples) is a function of correlation strength and sample size. This is found by permutations of the sample or the large sample limit of Equation 4 (again for τ_a) that follows the standard normal distribution.

$$z = \frac{\tau_a 3n(n-1)/2}{\sqrt{n(n-1)(2n+5)/2}} \tag{4}$$

2.2 Correlation Filter

With the drift-diffusion picture of Figure 1 in mind, possible UHECR deflections from a source are found by calculating energy-position correlations inside spherical cap sections, or "wedges," on a grid of points with an equal spacing of 2° within the field of view (FOV) [11].

These wedge bins are defined by a maximum radius δ_j from the grid point,i, (Equation 2) and the boundaries of two azimuths (Equation 5a). The azimuths go clockwise and a wedge pointed towards 90° supergalactic latitude (SGB) has an azimuth, ϕ, of zero and one pointed towards -90° SGB has a ϕ of 180°. The angular distance between the wedge pointing direction, ϕ_i, and an events azimuth is given by Equation 5b.

$$\phi_{ij} = \text{atan}\frac{\cos B_i \sin(L_i - L_j)}{\cos B_j \sin B_i - \sin B_j \cos B_i \cos(L_i - L_j)} \tag{5a}$$

$$\Delta\phi_{ij} = \text{mod}(|\phi_{ij} - \phi_i| + 180, 360) - 180 \tag{5b}$$

With this correlation filter shape four parameters must be scanned at every grid point to maximize the pre-trial significance. Though negative correlations are physically expected from magnetic deflections; the sign of the correlation, and its strength, are not scanned for nor restricted. The limits on these parameters are large to account for conceivable deflection scenarios and are the following:

1. Energy Threshold, E_i: 10 to 100 EeV, 5 EeV steps.
2. Wedge Angular Distance, D_i=max(δ_{ij}): 15° to 90°, 5° steps.
3. Wedge Direction, ϕ_i: 0° to 355°, 5° steps.
4. Wedge Width, $W_i = 2 * \text{max}(|\Delta\phi_{ij}|)$: 10° to 90°, 10° steps (5° on each side of ϕ_i).

Events are in the wedge if $E_j \geq E_i$ & $\delta_{ij} \leq D_i$ & $-W_i/2 \leq \Delta\phi_{ij} \leq W_i/2$ (i is the grid point index). The parameters (E_i, D_i, ϕ_i, and W_i) are chosen for the minimum energy-position correlation, $corr(\delta_{ij}, E_j)$, p-value (Equation 4).

The most significant correlation is at 18.3° SGB, -12.9° SGL and shown in Figure 2(a). With 29 events (E≥30 EeV) τ_b=−0.675 has pre-trial significance of 5.5σ. Figure 2(b) shows a scatter plot of energy versus angular distance and a linear fit (Equation 1a with Z=1) results in an estimate of $S*B$ = 49.24 kpc*μG. If the source is assumed to be at the distance to M82 (3.7 Mpc) the uniform magnetic field required to cause this deflection would be B=13 nG.

3 Simulations

Two Monte Carlo (MC) simulated event sets are used in this analysis. This first is an isotropic simulation assuming no specific sources or correlation with the supergalactic (or galactic) plane. The analysis is applied to isotropic simulations for the significance calculation of any anisotropy found as described further in Section 4. The second is a simple simulation of a supergalactic magnetic sheet resulting in an energy dependent diffusion of events away from the supergalactic plane. This is used to motivate the statistic that tests the hypothesis of supergalactic sources and magnetic fields; this test statistic is described in Section 4 and is searched for in the isotropic MC. These simulations can also be used as an estimate of the average uniform field strength between us and supergalactic sources.

3.1 Isotropic Simulation

Events are defined by energy, zenith angle, azimuthal angle, and trigger time. Latitude and longitude are the center of Telescope Array (39.3° Long., 112.9° Lat.). These horizontal coordinates are used to calculate the supergalactic longitude (SGL) and latitude (SGB) coordinates. Actual data coordinates are used for the isotropic simulations.

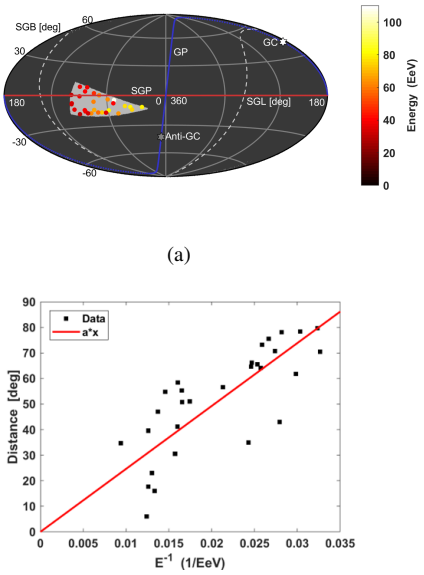

(a)

(b)

Figure 2. (a) Supergalactic Hammer-Aitoff projection of the maximum significance "wedge" at 18.3° SGB, -12.9° SGL. The correlation τ_b=−0.675 and with 29 data events has a pre-trial one-sided significance of 5.5σ. The energy threshold is E_i≥30 EeV, wedge width W_i=30°, angular distance D_i=80°, and direction ϕ_i=90°. (b) Scatter plot of $1/E$ versus angular distance δ in the wedge.

Energy spectrum detector biases are taken into account by interpolation sampling a large set of MC reconstructed through a surface detector simulation thrown with the HiRes/TA spectrum ([12], [13]). The same cuts as data are applied to these fully simulated events and there are 386,125 with energies E≥$10^{19.0}$ eV. The number of events in each isotropic MC event set is the same as data in each 5 EeV bin. Each set of isotropic MC events simulates the expected data given the detector configuration and on-time with no energy anisotropies.

3.2 Supergalactic Magnetic Sheet Simulation

A simple toy-model simulation of an intervening supergalactic magnetic sheet is made by embedding event deflections in supergalactic latitude (SGB), proportional to $1/energy$, for a fraction of events in isotropic simulations. The approximate apparent deflection from the source of a charged particle in a uniform magnetic field is shown in Equation 1a [9]. A supergalactic sheet simulation, with an F = 65.7% isotropic fraction (1988 out of 3027 events) and $S*B$=18.47 kpc$*\mu$G, is shown in Figure 3.

Unlike the isotropic simulations data coordinates are not used. To take into account the TA exposure on-time is simulated by sampling the trigger times of 264,499 data events with E>$10^{17.7}$ eV. The azimuthal angle distribution is uniform from 0° to 360° and the zenith angle distribution is g(θ) = sin(θ)cos(θ) due to the flat SD array.

The deflections δ_j are calculated for each MC event, j, assuming proton (Z=1) and an $S*B$; events with initial positive SGB have a positive deflection and a negative SGB have a negative deflection. Then the event positions, SGB_j, and energies, E_k, are decoupled into separate sets. The energies, E_k, and their deflection from SGB = 0 (δ_k) are assigned to the closest SGB_j value (min[δ_k-SGB_j]) in random order.

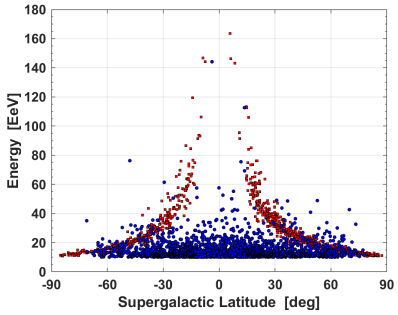

Figure 3. Toy-model supergalactic magnetic sheet simulation. Blue circles are the F = 65.7% isotropic fraction of MC events. Red squares are the anisotropic MC events magnetically diffused away from the supergalactic plane with $S*B$=18.47 kpc$*\mu$G. Overall, event positions are isotropic and the energy spectrum is created according to the published HiRes/TA result.

For any $S*B$ there will be a number of event positions that must be assigned isotropic energies due to the minimum deflection and the FOV. After the assignment of an SGB_j the energies, E_k, with a position-deflection error of $|SGB_j-\delta_k|>10°$ are put into the isotropic proportion. This allows some random noise in the simulation.

Event positions of SGB_j<min($|\delta_k|$) (the center of Figure 3), or $SGB_j>max(|\delta_k|)$ (the edges of Figure 3), are also part of the isotropic proportion. For larger isotropic total fractions, F, a random selection of energies and positions are taken from the anisotropic portion and randomized.

4 Supergalactic Structure

No single correlation tests the hypothesis that sources and magnetic fields are correlated with local large scale structure. And no single correlation can be significant when taking into account the >100,000 scan parameter combinations at all 6553 grid points. To test for supergalactic structure of multiplets the mean τ_b inside equal solid angle bins of angular distance (SGB_i) from the supergalactic plane are used. The pre-trial significance of the correlations are not used as they were scanned for. The correlation strength, τ_b, is used because it is not explicitly scanned for and contains more information by its sign (±).

The expectation is that negative correlations will be closer to the supergalactic plane. Furthermore, since negative correlations viewed from the opposite direction appear as a positive correlations ($(x_j, y_j) \rightarrow (x_j, -y_j)$), positive correlations are expected at large angular distances from the supergalactic plane. This is shown by a projection of the τ_b for the magnetic sheet simulation in Figure 4(a) and its averages τ_b in Figure 4(b).

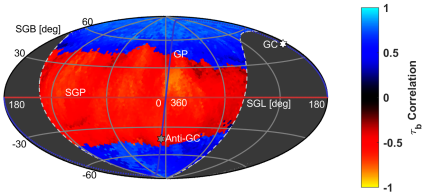

(a)

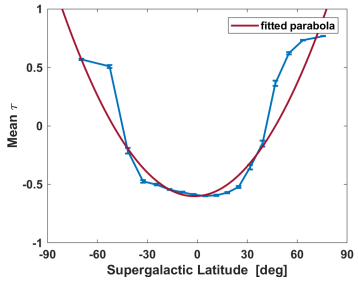

(b)

Figure 4. Supergalactic magnetic sheet simulation. (a) Projection of the correlation strength τ_b for all grid points. Solid curves indicate the galactic plane (GP) in blue and supergalactic plane (SGP) in red. (b) Mean τ_b inside equal solid angle bins for the supergalactic magnetic sheet simulation. The parabola shows the curvature parameter, a, chosen as the test statistic. a=2.5×10^{-4}.

4.1 Significance Test

The single parameter necessary to test the supergalactic structure of multiplets hypothesis is the curvature parameter, "a," of a parabolic fit ($ax^2 + bx + c$) to the mean τ_b in the supergalactic latitude bins shown in Figure 4(b). Due to the boundaries of $|\tau_b| \leq 1$ and $|SGB| < 90°$ greater correlation curvature, a, corresponds to a minimum closer to the supergalactic plane as shown in Figure 5. It also means that the minimum negative correlation, and maximum positive correlation, averages are larger in magnitude.

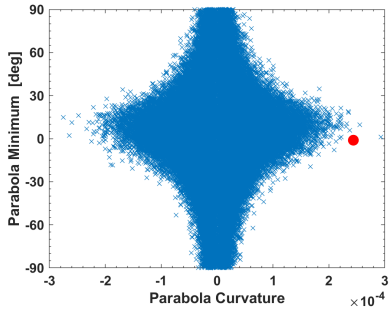

Figure 5. The correlation mean parabola fit curvature, as in Figure 4(b), versus minimum for 200,000 isotropic MC sets shows that a high curvature has a tendency for a minimum near the supergalactic plane. The red dot is the data result.

To calculate the data significance of a supergalactic structure of multiplets the analysis described above is applied, both to the data, and the isotropic MC sets. The number of MC sets with a correlation curvature, a, greater than the data gives the probability that there is not a supergalactic structure of multiplets.

5 Data Set

SD data recorded between May 11 of 2008 and 2015 is used for this analysis. The energy of reconstructed events is determined by the SD array and renormalized by 1/1.27 to match the calorimetrically determined fluorescence detector energy scale ([14]). The reconstruction of these events is the same as the "Hotspot" analysis of [15]. Due to the inclusion of lower energy events, down to $10^{19.0}$ eV, tighter data cuts are required for good zenith angle resolution.

After cuts, there are 3027 events in the data set. Events in the data set match the following criteria:

1. E≥$10^{19.0}$ eV (where detection efficiency is ∼100%).
2. At least four SDs triggered.
3. Zenith angle of arrival direction <55°.
4. Reconstructed pointing direction error <5°.
5. Shower core >1.2 km from array boundary.
6. Shower lateral distribution fit χ^2/dof<10.

The additional cuts on pointing direction error and boundary distance improve the agreement between the distribution of zenith angles compared to the geometrical zenith angle exposure g(θ) = sin(θ)cos(θ). The azimuthal angle distribution is in very good agreement with the theoretical flat distribution. The energy spectrum is also in good agreement with the published spectrum ([14],[16]).

The energy resolution and zenith angle resolution of events in the data set range from ∼10 to 15% and ∼1.0° to 1.5° respectively, depending on core distance from the array boundary and improve with increasing energy. These resolutions are sufficient to search for UHECR energy anisotropies.

6 Results

The resulting data energy-position correlations are shown in Figure 6(a). Individual correlations with the highest pretrial significance are negative which means that there is a trend for the angular distance to increase with decreasing energy. This is the expectation for a grid point that happens to be near a UHECR source of magnetically scattered events. It can be seen that the negative τ_b correlations appear well correlated with the supergalactic plane.

Figure 6(b) shows the mean τ_b correlation of the data inside equal solid angle bins parallel to the supergalactic plane. The parabola curvature test statistic is a=2.4×10^{-4} and the minimum is at −1.1 SGB. It can be seen that the data correlations have a very similar form to that of the supergalactic magnetic sheet simulation, shown in Figure 4(b), that has a slightly higher a=2.5×10^{-4} at −1.7 SGB.

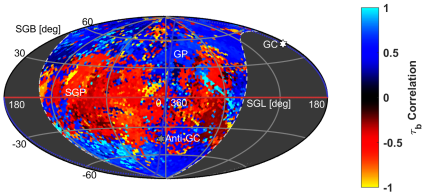

(a)

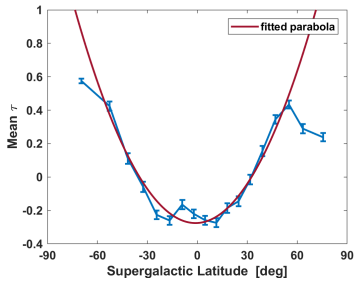

(b)

Figure 6. Data result. (a) Projection of the correlation strength τ_b for all grid points. Negative correlations expected for magnetic deflections are apparent around the supergalactic plane. Solid curves indicate the galactic plane (GP) in blue and supergalactic plane (SGP) in red. White and grey hexagrams indicate the Galactic center (GC) and anti-galactic center (Anti-GC) respectively. (b) Mean τ_b inside equal solid angle bins. The correlation curvature for the data is a=2.4×10^{-4}.

6.1 Significance of Correlation Curvature

By applying this analysis to isotropic MC sets and counting the number of MC with an a parameter greater than data (Figure 6(b)), the post-trial significance of the supergalactic structure of multiplets can be found. The resulting a distribution of 200,000 MC sets is shown in Figure 7. The number of MC sets created was limited by the computing time necessary for each simulation.

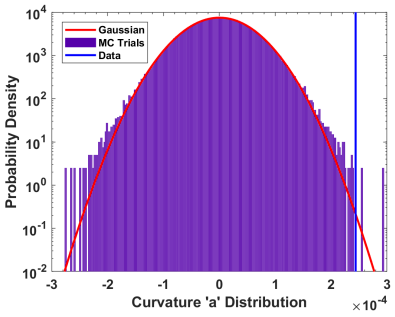

Figure 7. The distribution of the correlation curvature parameter a chosen as the supergalactic structure of multiplets test statistic for 200,000 isotropic MC sets. The purple bars are the MC PDF. The red line is a Gaussian distribution fit to the MC distribution. The data curvature is a=2.4×10^{-4} shown as a blue vertical line.

There are two MC sets with a larger curvature than data which gives a significance of 4.3±0.2σ. The area under the Gaussian fit from a=2.4×10^{-4} to a=∞ gives a significance of 4.6σ. Therefore, the resulting significance of a supergalactic structure of multiplets is about ~4.5σ.

6.2 Scan Parameter Distributions

Clues about UHECR sources, and intervening fields, may be found from the maximum significance wedge scan parameters of the apparent magnetic deflection multiplets. Due to the significance maximization there is a bias towards larger statistics so the data is compared to isotropic MC by taking the ratio of the parameter PDFs (Data/MC). PDF ratio plots for the wedge angular distance and energy threshold parameters are shown in Figure 8.

These ratios are for negative correlations at positions -40°<SGB_i<40° and have a linear fit to $1/E$ versus angular distance with an R^2>0. An R^2>0 is a better fit than a horizontal line and the $\delta \propto E$ model explains some of the variance. For data there are 2045 correlations used and greater than 3.99×10^8 for MC.

The data distributions of wedge angular distance, D, and width, W, do not show significant deviations from isotropy. The distribution of wedge pointing directions, Figure 8(a), indicates supergalactic structure with three deviations correlated with the supergalactic plane (SGP). Two peaks are approximately perpendicular to the SGP and one is parallel. This suggests diffusion of low energy events away from the supergalactic plane similar to the supergalactic magnetic sheet simulation. Three deviations of the energy threshold parameter are 35 EeV, 45 EeV, and 60 EeV. The last may correspond to the 57 EeV threshold of the TA hotspot analysis [15].

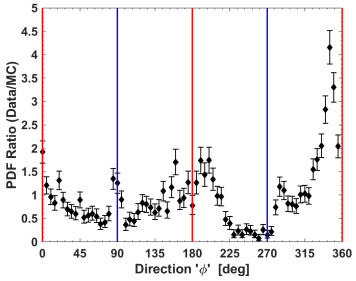

(a)

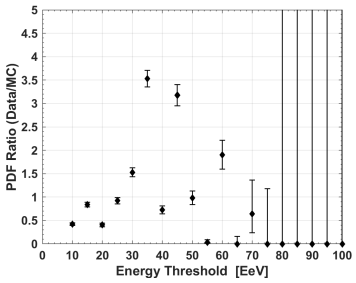

(b)

Figure 8. PDF ratio plot of scanned parameters. (a) Wedge pointing direction parameter, ϕ. Blue lines are perpendicular to the SGP and red lines are parallel. (b) Energy threshold, E. The three largest deviations are at 35 EeV, 45 EeV, and 60 EeV.

7 Summary

Intermediate-scale energy-position correlations inside spherical cap sections are shown to be correlated with the supergalactic plane. This structure has a $\sim 4.5\sigma$ significance using 7 years of Telescope Array SD data. This is possible evidence of large scale magnetic diffusion of ultra-high energy cosmic rays from their sources correlated with the local large scale structure. Confirmation of this result may be done once sufficient data is collected by the Telescope Array expansion to TAx4 [17].

References

[1] G. de Vaucouleurs, Astrophys. J. **202**, 610 (1975)

[2] A. Bonafede, L. Feretti, M. Murgia, F. Govoni, G. Giovannini, D. Dallacasa, K. Dolag, G.B. Taylor, Astron. Astrophys. **513**, A30 (2010), 1002.0594

[3] F. Nicastro, J. Kaastra, Y. Krongold, S. Borgani, E. Branchini, R. Cen, M. Dadina, C.W. Danforth, M. Elvis, F. Fiore et al., Nature **558**, 406 (2018)

[4] P.L. Biermann, H. Kang, D. Ryu, p. 9 p (1997), astro-ph/9709250

[5] D. Ryu, H. Kang, P.L. Biermann, Astron. Astrophys. **335**, 19 (1998), astro-ph/9803275

[6] Pierre Auger Collaboration, P. Abreu, M. Aglietta, E.J. Ahn, I.F.M. Albuquerque, D. Allard, I. Allekotte, J. Allen, P. Allison, J. Alvarez Castillo et al., Astropart. Phys. **35**, 354 (2012), 1111.2472

[7] A. Aab, P. Abreu, M. Aglietta, E.J. Ahn, I.A. Samarai, I.F.M. Albuquerque, I. Allekotte, J. Allen, P. Allison, A. Almela et al., EPJ C **75**, 269 (2015), 1410.0515

[8] H.P. Bretz, Ph.D. thesis, Rheinisch-Westphalian Technical University of Aachen (2011)

[9] P.G. Tinyakov, I.I. Tkachev, Astropart. Phys. **24**, 32 (2005), astro-ph/0411669

[10] M.G. Kendall, Biometrika **33**, 239 (1945)

[11] N.A. Teanby, Computers and Geosciences **32**, 1442 (2006)

[12] R.U. Abbasi et al. (HiRes), Phys. Rev. Lett. **100**, 101101 (2008), astro-ph/0703099

[13] D. Ivanov, Ph.D. thesis, Rutgers, the State University of New Jersey (2012), http://telescopearray.com/images/papers/theses/thesis_ivanov_rev2016.pdf

[14] T. Abu-Zayyad et al. (Telescope Array), Astrophys. J. **768**, L1 (2013), 1205.5067

[15] R.U. Abbasi et al. (Telescope Array), Astrophys. J. **790**, L21 (2014), 1404.5890

[16] R.U. Abbasi et al., Astropart. Phys. **68**, 27 (2015), 1410.3151

[17] H. Sagawa, *The Plan of the Telescope Array Experiment for the Next Five Years*, in *Proceedings, 33rd ICRC (ICRC2013): Rio de Janeiro, Brazil, July 2-9* (2013), p. 0121, http://www.cbpf.br/~icrc2013/papers/icrc2013-0121.pdf